

Simultaneous frequency stabilization of two 1550-nm lasers at single-photon level

Bo Yu(于波), Zhenqiang Yin(银振强), Weijie Ding(丁伟杰), Hui Yang(杨慧), and Weixin Liu(刘伟新)
Citation: Chin. Phys. B, 2026, 35 (**4**): 044208. DOI: 10.1088/1674-1056/ade072
http://cpb.iphy.ac.cn; http://iopscience.iop.org/cpb

What follows is a list of articles you may be interested in

Generation of stable and tunable optical frequency linked to a radio frequency by use of a high finesse cavity and its application in absorption spectroscopy

Yueting Zhou(周月婷), Gang Zhao(赵刚), Jianxin Liu(刘建鑫), Xiaojuan Yan(闫晓娟), Zhixin Li(李志新), Weiguang Ma(马维光), and Suotang Jia(贾锁堂)
Chin. Phys. B, 2022, 31 (**6**): 064206. DOI: 10.1088/1674-1056/ac4905

Spectral filtering of dual lasers with a high-finesse length-tunable cavity for rubidium atom Rydberg excitation

Yang-Yang Liu(刘杨洋), Zhuo Fu(付卓), Peng Xu(许鹏), Xiao-Dong He(何晓东), Jin Wang(王谨), and Ming-Sheng Zhan(詹明生)
Chin. Phys. B, 2021, 30 (**7**): 074203. DOI: 10.1088/1674-1056/abf91b

High-performance frequency stabilization of ultraviolet diode lasers by using dichroic atomic vapor spectroscopy and transfer cavity

Danna Shen(申丹娜), Liangyu Ding(丁亮宇), Qiuxin Zhang(张球新), Chenhao Zhu(朱晨昊), Yuxin Wang(王玉欣), Wei Zhang(张威), Xiang Zhang(张翔)
Chin. Phys. B, 2020, 29 (**7**): 074210. DOI: 10.1088/1674-1056/ab8c41

Stable continuous-wave single-frequency intracavity frequency-doubled laser with intensity noise suppressed in audio frequency region

Ying-Hao Gao(高英豪), Yuan-Ji Li(李渊骥), Jin-Xia Feng(冯晋霞), Kuan-Shou Zhang(张宽收)
Chin. Phys. B, 2019, 28 (**9**): 094204. DOI: 10.1088/1674-1056/ab327b

Non-crossover sub-Doppler DAVLL in selective reflection scheme

Lin-Jie Zhang(张临杰), Hao Zhang(张好), Yan-Ting Zhao(赵延霆), Lian-Tuan Xiao(肖连团), Suo-Tang Jia(贾锁堂)
Chin. Phys. B, 2019, 28 (**8**): 084211. DOI: 10.1088/1674-1056/28/8/084211

Simultaneous frequency stabilization of two 1550-nm lasers at single-photon level

Bo Yu(于波)[1,†], Zhenqiang Yin(银振强)[2,3,4,5], Weijie Ding(丁伟杰)[1], Hui Yang(杨慧)[1], and Weixin Liu(刘伟新)[1]

[1] *Department of Physics, Xinzhou Normal University, Xinzhou* 034000, *China*
[2] *CAS (Chinese Academy of Sciences) Key Laboratory of Quantum Information, University of Science and Technology of China, Hefei* 230026, *China*
[3] *CAS Center for Excellence in Quantum Information and Quantum Physics, University of Science and Technology of China, Hefei* 230026, *China*
[4] *Hefei National Laboratory, University of Science and Technology of China, Hefei* 230088, *China*
[5] *Anhui Province Key Laboratory of Quantum Network, University of Science and Technology of China, Hefei* 230026, *China*

(Received 21 April 2025; revised manuscript received 3 June 2025; accepted manuscript online 4 June 2025)

The twin-field quantum key distribution (TF-QKD) requires that two lasers hundreds of kilometers apart must have the same frequency to achieve the high single-photon interference visibility. This means that both lasers need to be stabilized to the same frequency reference. A simple and robust system is presented for simultaneously stabilizing two 1550-nm lasers at the single-photon level. By utilizing the single-photon multi-frequency modulation technology, both the fiber laser and distributed feedback (DFB) laser are stabilized to the π-phase shifted fiber Bragg grating at the same time. The frequency fluctuations of fiber laser and DFB laser are bounded within 1.39 MHz and 1.53 MHz over 2000 s, respectively. These two frequency-stabilized 1550-nm lasers could be used for TF-QKD.

Keywords: single-photon multi-frequency modulation, frequency stabilization, π-phase shifted fiber Bragg grating

PACS: 42.55.–f, 42.60.Fc, 42.79.Dj

DOI: 10.1088/1674-1056/ade072 **CSTR:** 32038.14.CPB.ade072

1. Introduction

The security of quantum key distribution (QKD) is guaranteed by the basic principles of quantum mechanics.[1–5] Now the QKD is currently in the stage of network construction, and the intercity networks require the long communication distance and high bit rate. The twin-field quantum key distribution (TF-QKD) is the most potential communication protocol at present because it could break through the QKD distance limit by measuring the single-photon interference at an untrusted intermediate node.[6] It is also immune to the side-channel attacks from single-photon detectors (SPDs), such as the measurement-device-independent quantum key distribution.[7–13]

Since Lucamarini *et al.* proposed the first TF-QKD protocol in 2017,[6] the TF-QKD has attracted the wide attention and many theoretical investigations have been carried out, such as phase-matching TF-QKD,[14] sending-or-not-sending TF-QKD,[15,16] no phase postselection TF-QKD,[17–19] and partial phase postselection TF-QKD.[20] At the same time, the experimental research has also developed rapidly. In 2019, Minder *et al.* demonstrated the feasibility of break through the key-rate limit without trusted relay by using the TF-QKD experimental demonstration.[21] In 2020, Chen *et al.* implemented TF-QKD with independent lasers over 509-km ultralow loss optical fiber by using the sending-or-not-sending protocol, and they also demonstrated that the TF-QKD is useful for the field implementation of intercity QKD.[22] Later they realized TF-QKD through sending-or-not-sending protocol with two lasers over a 511-km fiber linking the two distant metropolitan areas.[23] In 2023, Liu *et al.* demonstrated the fiber-based TF-QKD over 1002 km by using the 3-intensity sending-or-not-sending protocol.[24] In a word, the technical difficulty of TF-QKD is the precise manipulation of two-field single-photon interference. That is, it should keep the frequency, phase and polarization of twin-field single-photon signals hundreds of kilometers apart to be the same in order to achieve the high single-photon interference visibility.

Here, we focus on the frequency stabilization of two single-photon signals. The common Pound–Drever–Hall method[25–27] combined with optical amplifiers are often used to stabilize the two lasers to an ultra-stable Fabry–Perot (FP) cavity as the frequency reference for a TF-QKD system. However, the optical amplifiers could only amplify the laser signal at the classical laser intensity, and the multistage amplification would increase the system noise and costs. So this method may not be entirely suitable for the actual TF-QKD system. The soft-lock scheme[28] may be used for stabilizing the mul-

[†]Corresponding author. E-mail: yb@xztu.edu.cn

© 2026 Chinese Physical Society and IOP Publishing Ltd. All rights, including for text and data mining, AI training, and similar technologies, are reserved.

tiple lasers by comparing the dip position differences between the reference laser and unlocked lasers with the preset offsets. But it is invalid at the single-photon level because the reflected single-photon signal of the FP cavity cannot be effectively extracted from the random quantum noise. The π phase-shifted fiber Bragg grating (PSFBG) has a stable Bragg frequency due to its small size and easy isolation of external environmental noise through the tight packaging. Thus the PSFBG could be used as the optical frequency reference.[29] Taking into account the photothermal effect from the classical laser inducing the PSFBG frequency shift,[30,31] the frequency stabilizing scheme must be implemented at the single-photon level in order to eliminate the photothermal effect of PSFBG.[32]

This paper presents a simple and robust system for simultaneous stabilization of two 1550-nm lasers at the single-photon level. The input laser is attenuated to the single-photon level while single-photon signals also eliminate the photothermal effect of PSFBG. By applying the single-photon multi-frequency modulation technology, the signal-to-noise ratio (SNR) of modulated single-photon counting is improved and both the fiber laser and DFB laser are simultaneously stabilized to the PSFBG at the single-photon level.

2. Single-photon multi-frequency modulation technology

The single-photon multi-frequency modulation technology simultaneously modulates the output frequency of multiple lasers by using multiple radiofrequency signals, and obtains the corresponding error signal through the independent demodulation. Thus multiple lasers could be simultaneously locked to a frequency reference. This technology is divided into four steps. The first step is to simultaneously modulate multiple laser signals in high-frequency band. As is known to all, the random single photon signals without modulation follow the uniform distribution in the time domain. Correspondingly, its frequency spectrum exhibits a white noise distribution. When the output frequencies of multiple lasers are simultaneously modulated with several independent cosine waves and combined together, the total output frequency at time t is

$$\nu(t) = \sum_i [\nu_i + m_i \cos(2\pi f_i t)], \tag{1}$$

where ν_i ($i = 1, 2, \ldots$) is the i-th laser frequency without modulation, and m_i ($i = 1, 2, \ldots$) is the i-th modulation amplitude for the i-th modulation frequency f_i ($i = 1, 2, \ldots$).

The second step is to convert the frequency modulation of multiple lasers into single-photon counting modulation. When the multiple laser signals are transmitted through the single frequency reference, the detection probability of single photon signals coincide the cosine waves. During the sample time T, the effective counting rate $r_T(t)$ is

$$r_T(t) = \sum_i \left\{ r_i + a_i \left[\frac{\sin(\pi f_i T)}{\pi f_i T} \right] \cos(2\pi f_i t + \pi f_i T) \right\}, \tag{2}$$

where r_i ($i = 1, 2, \ldots$) is the i-th average detection probability, and a_i ($i = 1, 2, \ldots$) is the i-th modulation depth for the i-th modulation frequency f_i ($i = 1, 2, \ldots$). The effective counting rate is also modulated with multiple frequencies. After the several single photon signals are converted to transistor–transistor logic (TTL) pulses, the distribution of TTL pulses in the time domain contains the multi-frequency modulation information.

The third step is to obtain the error signal by independent demodulation. One lock-in amplifier (LIA) could only extract the amplitude and phase information of the useful signal at the i-th modulation frequency f_i ($i = 1, 2, \ldots$) within the filter bandwidth and reject the noise signal outside the filter bandwidth. After the modulated TTL pulses transmitted through the mixer and low-pass filter, the LIA output for the i-th modulation frequency f_i ($i = 1, 2, \ldots$) is

$$V_{\text{sig}} V_{\text{ref}} \approx \frac{1}{2} a_i \frac{\mathrm{d}V_{\text{sig}}}{\mathrm{d}\nu} \cos\varphi, \tag{3}$$

where V_{sig} is the analog signal amplitude corresponding to the TTL pulses, V_{ref} and φ are the amplitude and phase of reference signal for the i-th modulation frequency f_i ($i = 1, 2, \ldots$), respectively. The phase-sensitive detection for each modulation frequency is realized. So the SNR of modulated single-photon counting is boosted and the corresponding error signal is obtained.

The fourth step is frequency stabilization of multiple lasers. The several error signals are optimized by adjusting their intensity and response time and then independently injected into the frequency control port of the corresponding laser. Finally the multiple lasers could be simultaneously stabilized to the same frequency reference.

3. Experiments

The whole locking system can be divided into the locking part of the fiber laser (NKT Photonics, Koheras Adjustik E15) and the locking part of the distributed feedback (DFB) laser (Teraxion, PureSpectrum-LM), as shown in Fig. 1. Both the fiber laser and DFB laser operating at 1550-nm wavelength with 40-mW output power emit the linearly polarized laser signal aligned to the slow axis of the polarization maintain fiber. The isolators are used to block the reflected signals from the other optical components. The attenuators are used to reduce the each laser intensity to the single-photon level with about 0.1 photons per detection gate of the SPD (Quantum, QCD-300), while single-photon signals also eliminate the photothermal effect of PSFBG (Teraxion, TFN). The fiber laser and the DFB laser are independently modulated using the modulation

signals with different frequencies. When the two single photon signals are combined and transmitted through the PSFBG, the single-photon frequency modulation is transformed into the single-photon detection probability modulation. After the single-photon signals are detected by the gated SPD, the distribution of output TTL signals in the time domain contains the information of two modulation frequencies.

Here, the working temperature of PSFBG is controlled by using an active temperature feedback system. The temperature stability of PSFBG is further improved by placing the PSFBG in a temperature control box. The notch bandwidth and rejection bandwidth of PSFBG are 38 MHz and 250.8 GHz, respectively. The insertion loss of PSFBG is 0.9 dB. The center wavelength of PSFBG is 1550 nm and the whole frequency tuning range is ±20 GHz. The 38-MHz transmission peak for the slow axis of PSFBG is used as the optical frequency reference.

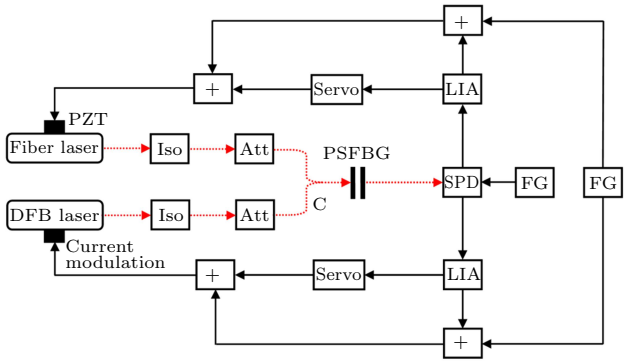


Fig. 1. Schematic diagram of the two 1550-nm lasers stabilized to the PSFBG (red dashed lines for the light signal, black solid lines for the electrical signal). PZT: piezoelectric transducer; Iso: isolator; Att: attenuator; C: coupler; PSFBG: π-phase-shifted fiber Bragg grating; SPD: single-photon detector; FG: function generator; LIA: lock-in amplifier; +: adder.

For acquiring the independent error signal, it is necessary to set the optimal filter bandwidth and modulation frequency, which ensures that one error signal could not contain the other modulation information and the corresponding SNR is maximized.

For the fiber laser, the integration time and filter slope of LIA (Stanford Research Systems, SR830) are 300 μs and 24 dB respectively, and the equivalent filter bandwidth is 0.26 kHz. For the DFB laser, the integration time and filter slope of another LIA (Stanford Research Systems, SR830) are 100 μs and 12 dB, respectively, so the equivalent filter bandwidth is 1.25 kHz. The modulation frequency for the fiber laser and DFB laser are 9 kHz and 80 kHz respectively, which can avoid the influence of flicker noise in the low frequency band. The frequency spacing between two modulation frequencies is 71 kHz, which is ten times larger than either filter bandwidth. So the each LIA could only extract the useful signals for its own modulation frequency and suppress the noise signals outside the filter bandwidth. For the fiber laser, the corresponding error signal is firstly optimized by a servo system and later injected to the piezoelectric transducer port to change the cavity length for adjusting the output wavelength. For the DFB laser, the corresponding error signal is also optimized by another servo system and then loaded to the current modulation port to control the laser wavelength. Finally both the fiber laser and DFB laser are stabilized to the PSFBG simultaneously.

4. Results and discussion

We first measure the transmission signal of both lasers, and then analyze the error signal and frequency locking results of both lasers. The transmission signal of both lasers are measured using the two ramp signals to independently scan the fiber laser and DFB laser under the classical light at the same time, as shown in Fig. 2.

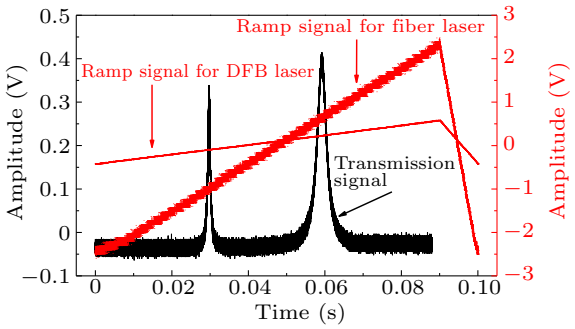


Fig. 2. Transmission signal and ramp signal for the fiber laser and DFB laser. The vertical axis on the left and right depicts the amplitude of transmission signal and ramp signal, respectively. The two red lines represent the two ramp signals for the fiber laser and DFB laser, respectively. The two peaks with black colored line are the corresponding transmission signal for the fiber laser and DFB laser, respectively.

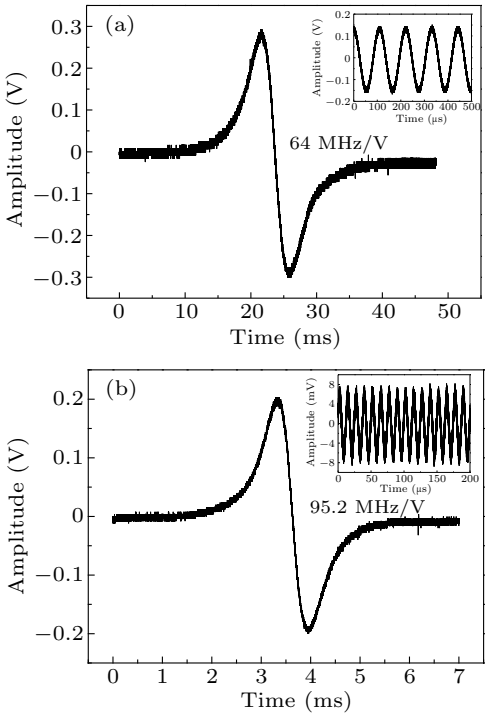


Fig. 3. (a) Error signal for the fiber laser and the inset is the corresponding modulation signal. (b) Error signal for the DFB laser and the inset is the corresponding modulation signal.

The single-photon multi-frequency modulation technology is used to simultaneously stabilize the fiber laser and DFB laser to the PSFBG. For the fiber laser, the error signal is displayed in Fig. 3(a) with the SNR being 25. The linear slope for optical frequency versus amplitude is 64 MHz/V. For the DFB laser, the error signal is shown in Fig. 3(b) with the SNR being 33. The linear slope for optical frequency versus amplitude is 95.2 MHz/V. The above two error signals are effective for stabilizing two 1550-nm lasers at the same time.

The frequency stabilization results of fiber laser are presented in Fig. 4. As depicted in Fig. 4(a), the free running fiber laser exhibits a significant random frequency drift exceeding 38 MHz. However, when the negative feedback system is employed, it effectively suppresses the frequency drift of the fiber laser. The statistics of locked error signal is fitted by using a Gaussian function, as illustrated in Fig. 4(b). The full width at half maximum (FWHM) of locked error signal is 1.39 MHz, indicating that the stabilized fiber laser maintains its frequency within a bounded range of 1.39 MHz over the duration of 2000 s.

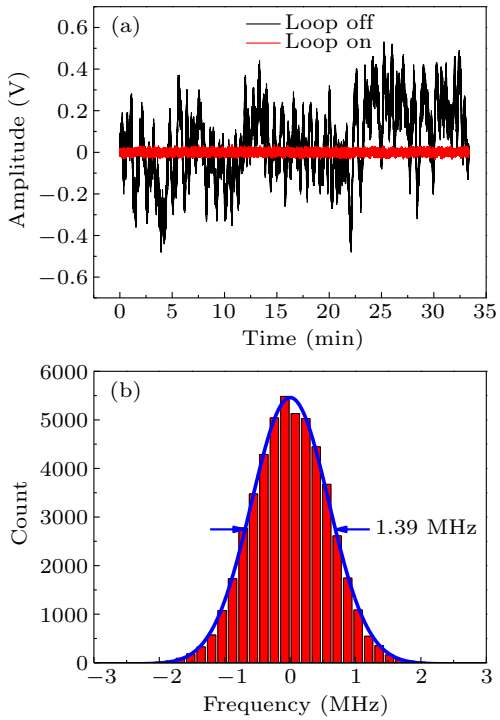


Fig. 4. (a) Frequency stabilization results for the fiber laser with feedback loop on or off. (b) Statistics of the locked error signal.

The frequency stabilization results of DFB laser are presented in Fig. 5. As depicted in Fig. 5(a), the free running DFB laser exhibits a significant frequency drift exceeding 38 MHz. However, the frequency drift of the DFB laser is effectively suppressed with the implementation of a feedback loop. Furthermore, the statistical analysis reveals that the locked error signal conforms to a Gaussian distribution, as illustrated in Fig. 5(b). The FWHM of the locked error signal is measured to be 1.53 MHz, indicating that the stabilized DFB laser experiences a bounded frequency drift within 1.53 MHz over the duration of 2000 s. Remarkably, despite encountering the temperature fluctuations and mechanical vibrations, both frequency stabilization systems for the two 1550-nm lasers perform admirably and result in the significantly improved long-term frequency stability.

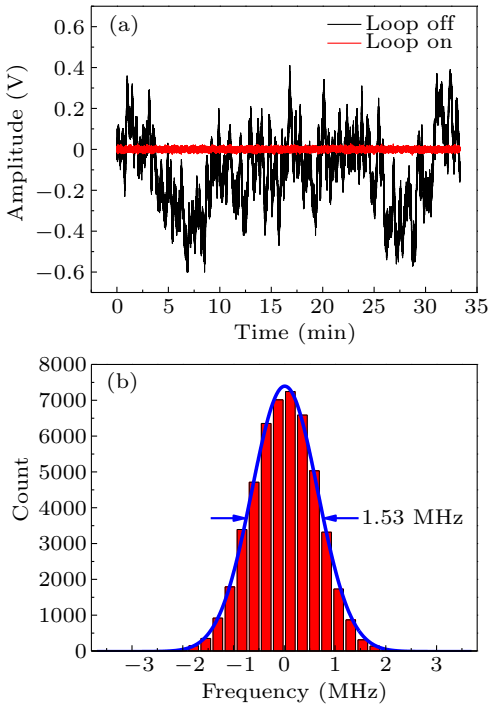


Fig. 5. (a) Frequency stabilization results for the DFB laser with feedback loop on or off. (b) Statistics of the locked error signal.

5. Conclusion

In conclusion, we have shown a simple and robust system for simultaneous frequency stabilization of two 1550-nm lasers. By use of the single-photon multi-frequency modulation technology, both the fiber laser and DFB laser are simultaneously stabilized to the PSFBG at the single-photon level. The frequency fluctuations of fiber laser and DFB laser are bounded within 1.39 MHz and 1.53 MHz over 2000 s, respectively. The advantages for our system are as follows: (i) these two 1550-nm lasers are directly stabilized at the single-photon level by utilizing the single-photon multi-frequency modulation technology; (ii) this single-photon multi-frequency modulation technology is a general method and it could also be used for phase or polarization stabilization of multiple lasers at the same time; (iii) these two 1550-nm frequency-stabilized lasers could be applied for TF-QKD.

Acknowledgements

Project supported by the Fundamental Research Program of Shanxi Province, China (Grant No. 202403021211084) and the Science and Technology Program of Xinzhou City, Shanxi Province, China (Grant No. 20240509).

References

[1] Ekert A K 1991 *Phys. Rev. Lett.* **67** 661
[2] Lütkenhaus N and Shields A J 2009 *New J. Phys.* **11** 045005
[3] Scarani V, Bechmann-Pasquinucci H, Cerf N J, Dušek M, Lütkenhaus N and Peev M 2009 *Rev. Mod. Phys.* **81** 1301
[4] Xu F H, Ma X F, Zhang Q, Lo H K and Pan J W 2020 *Rev. Mod. Phys.* **92** 025002
[5] Portmann C and Renner R 2022 *Rev. Mod. Phys.* **94** 025008
[6] Lucamarini M, Yuan Z L, Dynes J F and Shields A J 2018 *Nature* **557** 400
[7] Lo H K, Curty M and Qi B 2012 *Phys. Rev. Lett.* **108** 130503
[8] Ma X F and Razavi M 2012 *Phys. Rev. A* **86** 062319
[9] Tang Y L, Yin H L, Chen S J, Liu Y, Zhang W J, Jiang X, Zhang L, Wang J, You L X, Guan J Y, Yang D X, Wang Z, Liang H, Zhang Z, Zhou N, Ma X, Chen T Y, Zhang Q and Pan J W 2015 *IEEE J. Sel. Topics Quantum Electron.* **21** 6600407
[10] Tang Z, Wei K, Bedroya O, Qian L and Lo H K 2016 *Phys. Rev. A* **93** 042308
[11] Yin H L, Chen T Y, Yu Z W, Liu H, You L X, Zhou Y H, Chen S J, Mao Y, Huang M Q, Zhang W J, Chen H, Li M J, Nolan D, Zhou F, Jiang X, Wang Z, Zhang Q, Wang X B and Pan J W 2016 *Phys. Rev. Lett.* **117** 190501
[12] Wang C, Yin Z Q, Wang S, Chen W, Guo G C and Han Z F 2017 *Optica* **4** 1016
[13] Liu J Y, Ma X, Ding H J, Zhang C H, Zhou X Y and Wang Q 2023 *Phys. Rev. A* **108** 022605
[14] Ma X F, Zeng P and Zhou H Y 2018 *Phys. Rev. X* **8** 031043
[15] Wang X B, Yu Z W and Hu X L 2018 *Phys Rev. A* **98** 062323
[16] Yu Z W, Hu X L, Jiang C, Xu H and Wang X B 2019 *Sci. Rep.* **9** 3080
[17] Lin J and Lütkenhaus N 2018 *Phys. Rev. A* **98** 042332
[18] Cui C, Yin Z Q, Wang R, Chen W, Wang S, Guo G C and Han Z F 2019 *Phys. Rev. Appl.* **11** 034053
[19] Curty M, Azuma K and Lo H K 2019 *Quantum Inf.* **5** 64
[20] Zhou Y, Yin Z Q, Wang R Q, Wang S, Chen W, Guo G C and Han Z F 2022 *Phys. Rev. Appl.* **18** 054026
[21] Minder M, Pittaluga M, Roberts G L, Lucamarini M, Dynes J F, Yuan Z L and Shields A J 2019 *Nat. Photon.* **13** 334
[22] Chen J P, Zhang C, Liu Y, Jiang C, Zhang W, Hu X L, Guan J Y, Yu Z W, Xu H, Lin J, Li M J, Chen H, Li H, You L, Wang Z, Wang X B, Zhang Q and Pan J W 2020 *Phys. Rev. Lett.* **124** 070501
[23] Chen J P, Zhang C, Liu Y, Jiang C, Zhang W J, Han Z Y, Ma S Z, Hu X L, Li Y H, Liu H, Zhou F, Jiang H F, Chen T Y, Li H, You L X, Wang Z, Wang X B, Zhang Q and Pan J W 2021 *Nat. Photon.* **15** 570
[24] Liu Y, Zhang W J, Jiang C, Chen J P, Zhang C, Pan W X, Ma D, Dong H, Xiong J M, Zhang C J, Li H, Wang R C, Wu J, Chen T Y, You L, Wang X B, Zhang Q and Pan J W 2023 *Phys. Rev. Lett.* **130** 210801
[25] Black E D 2001 *Am. J. Phys.* **69** 79
[26] Han C Y, Zhou M, Gao Q, Li S Y, Zhang S, Qiao H, Ai D, Zhang M Y, Lou G, Luo L M and Xu X Y 2018 *Laser Phys. Lett.* **15** 045702
[27] Zeng Y, Wang K P, Liu Y Y, He X D, Liu M, Xu P, Wang J and Zhan M S 2018 *J. Opt. Soc. Am. B* **35** 454
[28] Wang D Y, Bu W H, Xie D Z, Chen T and Yan B 2018 *J. Opt. Soc. Am. B* **35** 1658
[29] Cliché J F, Painchaud Y, Latrasse C, Picard M J, Alexandre I and Têtu M 2007 *OSA Technical Digest paper* BTuE2
[30] Chow J H, Sheard B S, McClelland D E and Gray M 2005 *Opt. Lett.* **30** 708
[31] Ding M, Chen D J, Fang Z J, Wang D, Zhang X, Wei F, Yang F, Ying K and Cai H W 2016 *Opt. Express* **24** 25370
[32] Yu B, Hu J Y, Jing M Y, Zhang G F, Xiao L T and Jia S T 2016 *Laser Phys.* **26** 105104